

Syntheses, Structural Determinations of $[\text{Ru}(\text{ROCS}_2)_2(\text{PPh}_3)_2]^{+0}$ Pairs, and Kinetic Analyses of Thermal Reactions Involving Transient $\text{trans}-[\text{Ru}(\text{PrOCS}_2)_2(\text{PPh}_3)_2]$ Species ($\text{ROCS}_2^- = \text{Ethyl- or Isopropylthiocarbonate and PPh}_3 = \text{Triphenylphosphine}$)

Kyoko Noda,[†] Yuko Ohuchi,[†] Akira Hashimoto,[†] Masayuki Fujiki,[†] Sumitaka Itoh,[†] Satoshi Iwatsuki,[‡] Toshiaki Noda,[†] Takayoshi Suzuki,^{*§} Kazuo Kashiwabara,[†] and Hideo D. Takagi^{*†}

Graduate School of Science and Research Center for Materials Science, Nagoya University, Furocho, Chikusa, Nagoya 464-8602, Japan, Department of Chemistry, Waseda University, Ookubo, Shinjuku 169-8555, Japan, and Department of Chemistry, Graduate School of Science, Osaka University, Toyonaka 560-0043, Japan

Received August 31, 2005

Controlled-potential electrochemical oxidation of $\text{cis}-[\text{Ru}(\text{ROCS}_2)_2(\text{PPh}_3)_2]$ ($\text{R} = \text{Et, Pr}$) yielded corresponding Ru(III) complexes, and the crystal structures of $\text{cis}-[\text{Ru}(\text{ROCS}_2)_2(\text{PPh}_3)_2]$ and $\text{trans}-[\text{Ru}(\text{ROCS}_2)_2(\text{PPh}_3)_2](\text{PF}_6)$ were determined. Both pairs of complexes exhibited almost identical coordination structures. The Ru–P distances in $\text{trans}-[\text{Ru}^{\text{III}}(\text{ROCS}_2)_2(\text{PPh}_3)_2](\text{PF}_6)$ [2.436(3)–2.443(3) Å] were significantly longer than those in $\text{cis}-[\text{Ru}^{\text{II}}(\text{ROCS}_2)_2(\text{PPh}_3)_2]$ [2.306(1)–2.315(2) Å]: the smaller ionic radius of Ru(III) than that of Ru(II) stabilizes the trans conformation for the Ru(III) complex due to the steric requirement of bulky phosphine ligands while mutual trans influence by the phosphine ligands induces significant elongation of the Ru^{III}–P bonds. Cyclic voltammograms of the $\text{cis}-[\text{Ru}(\text{ROCS}_2)_2(\text{PPh}_3)_2]$ and $\text{trans}-[\text{Ru}(\text{ROCS}_2)_2(\text{PPh}_3)_2]^+$ complexes in dichloromethane solution exhibited typical dual redox signals corresponding to the $\text{cis}-[\text{Ru}(\text{ROCS}_2)_2(\text{PPh}_3)_2]^{+0}$ (ca. +0.15 and +0.10 V vs ferrocenium/ferrocene couple for $\text{R} = \text{Et}$ and Pr , respectively) and to $\text{trans}-[\text{Ru}(\text{ROCS}_2)_2(\text{PPh}_3)_2]^{+0}$ (–0.05 and –0.15 V vs ferrocenium/ferrocene for $\text{R} = \text{Et}$ and Pr , respectively) couples. Analyses on the basis of the Nicholson and Shain's method revealed that the thermal disappearance rate of transient $\text{trans}-[\text{Ru}(\text{ROCS}_2)_2(\text{PPh}_3)_2]$ was dependent on the concentration of PPh_3 in the bulk: the rate constant for the intramolecular isomerization reaction of $\text{trans}-[\text{Ru}(\text{PrOCS}_2)_2(\text{PPh}_3)_2]$ was determined as $0.338 \pm 0.004 \text{ s}^{-1}$ at 298.3 K ($\Delta H^\ddagger = 41.8 \pm 1.5 \text{ kJ mol}^{-1}$ and $\Delta S^\ddagger = -114 \pm 7 \text{ J mol}^{-1} \text{ K}^{-1}$), while the dissociation rate constant of coordinated PPh_3 from the $\text{trans}-[\text{Ru}(\text{PrOCS}_2)_2(\text{PPh}_3)_2]$ species was estimated as $0.113 \pm 0.008 \text{ s}^{-1}$ at 298.3 K ($\Delta H^\ddagger = 97.6 \pm 0.8 \text{ kJ mol}^{-1}$ and $\Delta S^\ddagger = 64 \pm 3 \text{ J mol}^{-1} \text{ K}^{-1}$), by monitoring the EC reaction (electrode reaction followed by chemical processes) at different concentrations of PPh_3 in the bulk. It was found that the trans to cis isomerization reaction takes place via the partial dissociation of PrOCS_2^- from Ru(II), contrary to the previous claim that it takes place by the twist mechanism.

Introduction

Historically, the trans influence by which a metal to ligand bond trans to the particular donor atom suffers from elongation has been suggested to be related to the ground-state property inherent in such complexes, while the trans effect by which lability of a ligand trans to a particular donor

atom increases has been related to both ground-state and transition-state characteristics.^{1,2} Therefore, trans influence and trans effect are not necessarily related to each other: to understand these two phenomena it is necessary to examine the metal–ligand bond lengths and lability of metal complexes with a series of ligands possessing different donor/acceptor properties.

* To whom correspondence should be addressed. E-mail: suzuki@chem.sci.osaka-u.ac.jp (T.S.), H.D.Takagi@nagoya-u.jp (H.D.T.).

[†] Nagoya University.

[‡] Waseda University.

[§] Osaka University.

(1) Greenwood, N. N.; Earnshaw, A. *Chemistry of the Elements*, 2nd ed.; Butterworth-Heinemann: Oxford, U.K., 1997.

(2) Huheey, J. E. *Inorganic Chemistry*, 2nd ed.; Harper & Row: New York, 1978.

We have recently reported a series of studies concerning the trans influence and trans effect in various $[\text{Co}(\text{dtc})_2(\text{P-ligand})_2]^+$ complexes ($\text{dtc}^- = N,N$ -dimethyldithiocarbamate and P-ligand = unidentate ligand with a phosphorus donor atom),^{3,4} in which we pointed out that the simple parametric descriptions of the donor and acceptor properties of P-ligands postulated by Giering and co-workers⁵ cannot explain the strengths of various $\text{Co}^{\text{III}}-\text{P}$ bonds estimated from the spectrophotometric method. To extend understandings of the effect by spectator ligands as well as the nature of phosphorus ligands, we examined the structures and isomerization reactions of $[\text{Ru}(\text{ROCS}_2)_2(\text{PPh}_3)_2]^{+0}$ complexes in this study, the former of which has never been reported in previous studies.⁶

As for the reactions of $[\text{Ru}/\text{Os}(\text{ROCS}_2)_2(\text{PPh}_3)_2]$ complexes,^{6,7} Chakravorty and co-workers reported "probable" cis to trans isomerization rate constant, and they claimed that the reaction proceeds through the twist mechanism. However, a calculation on the basis of the AOM (angular overlap model) indicates that the twist mechanism is not likely to take place for second- and third-row transition metal complexes with large ligand fields.^{3,4} In addition, our previous results for Co(III) species^{3,4} strongly indicate that the dissociation of coordinated ligands is significant even for d^6 -Ru(II) species, by considering the trans influence/trans effect of PPh_3 and the effect of the spectator ligand. Therefore, it is necessary to reinvestigate the reactions in more detail so as to determine the exact reaction mechanism.

In this article, (1) we report successful isolation and crystal structures of both d^5 -Ru(III) and d^6 -Ru(II) complexes for the first time and (2) the trans to cis isomerization process in the Ru(II) species was reanalyzed as the EC reaction by varying the concentration of PPh_3 in the bulk. The structures and reactivity of the d^5 -Ru(III) and d^6 -Ru(II) species were discussed on the basis of the trans influence/trans effect of the phosphine ligand.

Experimental Section

$[\text{Ru}(\text{ROCS}_2)_2(\text{PPh}_3)_2]$. The crude compounds were prepared by the literature method.^{6,8} The resulting EtOCS_2 complex, $[\text{Ru}(\text{EtOCS}_2)_2(\text{PPh}_3)_2]$, was recrystallized by the vapor phase diffusion of diethyl ether into dichloromethane solution, affording orange plate crystals. Anal. Calcd for $\text{C}_{42}\text{H}_{40}\text{O}_2\text{S}_4\text{P}_2\text{Ru}$: C, 58.11; H, 4.64. Found: C, 58.04; H, 4.50. $^1\text{H NMR}$ (CDCl_3 , 303 K, 400 MHz): δ 1.22 (t, $-\text{CH}_3$), 4.25 (q, $-\text{CH}_2-$), and 7.08–7.24 (m, $-\text{C}_6\text{H}_5$). UV–vis (CH_2Cl_2 , rt (room temperature), λ_{max}): 376 nm. Red block crystals of the $^i\text{PrOCS}_2$ complex, $[\text{Ru}(^i\text{PrOCS}_2)_2(\text{PPh}_3)_2]$, were obtained by recrystallization from dichloromethane/acetone/nitrile/

diethyl ether. Anal. Calcd for $\text{C}_{44}\text{H}_{44}\text{O}_2\text{S}_4\text{P}_2\text{Ru}$: C, 58.97; H, 4.95. Found: C, 59.26; H, 4.95. $^1\text{H NMR}$ (CDCl_3 , 303 K, 400 MHz): δ 1.17–2.26 (m, $-\text{CH}_3$), 5.16 (m, $-\text{CH}-$), and 7.07–7.23 (m, $-\text{C}_6\text{H}_5$). UV–vis (CH_2Cl_2 , rt, λ_{max}): 376 nm.

$[\text{Ru}(\text{ROCS}_2)_2(\text{PPh}_3)_2](\text{PF}_6)$. The crude EtOCS_2 complex was prepared by the modification of the reported method⁶ as follows: recrystallized $[\text{Ru}(\text{EtOCS}_2)_2(\text{PPh}_3)_2]$ was dissolved in acetone containing 0.1 mol kg^{-1} NH_4PF_6 , and electrolytically oxidized at 1.41 V vs ferrocenium/ferrocene couple by using a carbon fiber electrode as the anode. After completion of the electrolysis solvent was removed under reduced pressure, and an excess amount of aqueous NH_4PF_6 solution was added. The product was filtered and washed with water. The resulting crude green solid was recrystallized from dichloromethane/diethyl ether. Anal. Calcd for $\text{C}_{45.7}\text{H}_{47.4}\text{O}_2\text{S}_4\text{P}_3\text{RuF}_6\text{Cl}_{7.4}$ ($[\text{Ru}(\text{EtOCS}_2)_2(\text{PPh}_3)_2](\text{PF}_6) \cdot 3.7\text{CH}_2\text{Cl}_2$): C, 41.35; H, 3.60. Found: C, 41.21; H, 3.40. UV–vis (CH_2Cl_2 , rt, λ_{max}): 731, 445, 367, and ~ 250 nm.

$[\text{Ru}(^i\text{PrOCS}_2)_2(\text{PPh}_3)_2](\text{PF}_6)$. was obtained by the reaction of the Ru(II) complex with Ce(IV). To a solution containing 0.2 mol of $[\text{Ru}(^i\text{PrOCS}_2)_2(\text{PPh}_3)_2]$ and 2.18 mol of NH_4PF_6 in acetone/dichloromethane (5:1 v/v) was added 30 mL of aqueous solution of ceric ammonium nitrate (50 mmol kg^{-1}), and the mixture was stirred for 10 min. The crude product was filtered out and washed with water. Deep green crystals were obtained by recrystallization of the crude product from dichloromethane/diethyl ether. Anal. Calcd for $\text{C}_{44}\text{H}_{46}\text{O}_3\text{S}_4\text{P}_3\text{F}_6\text{Ru}$ ($[\text{Ru}(^i\text{PrOCS}_2)_2(\text{PPh}_3)_2](\text{PF}_6) \cdot \text{H}_2\text{O}$): C, 49.90; H, 4.38. Found: C, 50.05; H, 4.16. UV–vis (CH_2Cl_2 , rt, λ_{max}): 734, ~ 555 , 455, 369, and ~ 250 nm.

Other Chemicals. Triphenylphosphine, PPh_3 , was recrystallized twice from methanol/diethyl ether and dried under vacuum for 10 h at 70 °C. Tetra-*n*-butylammonium hexafluorophosphate, TBAF_6 , was recrystallized 3 times from ethanol/water and dried at 100 °C for 10 h in a vacuum oven. Dichloromethane, which was used as the solvent, was dried over molecular sieves 4A, followed by distillation.

Crystallography.⁸ The X-ray diffraction data for the EtOCS_2 complexes were collected at 23 °C on an automated Rigaku AFC-5R four-circle diffractometer. On the other hand, the data for the $^i\text{PrOCS}_2$ complexes were obtained at $-73(2)$ °C on a Rigaku Raxis-rapid imaging plate detector. A graphite-monochromated Mo $K\alpha$ radiation ($\lambda = 0.71073$ Å) was used for all measurements. The structures were solved by the direct method using SIR92 program⁹ and refined on F^2 (with all independent reflections) using the SHELXL97 program.¹⁰ All non-hydrogen atoms were refined anisotropically, and H atoms were introduced theoretically and treated by riding models, except for those of the solvent molecules of crystallization in $[\text{Ru}(^i\text{PrOCS}_2)_2(\text{PPh}_3)_2](\text{PF}_6) \cdot 0.5\text{CH}_2\text{Cl}_2 \cdot 0.5\text{CH}_3\text{CN}$.⁸

The crystallographic data are summarized in Table 1.

Spectrometric and Electrochemical Measurements. $^1\text{H NMR}$ spectra of samples in deuterated chloroform solution were recorded by a Bruker AMX-400WB spectrometer. The UV–vis absorption spectra were recorded by a Jasco V-570 spectrophotometer.

An attempt to estimate the rates for isomerization reactions by means of the stopped-flow method was not successful: the spectral change was too small for the reliable determination of the isomerization rate constants. In addition, it was hardly possible to isolate redox and following isomerization processes after complete redox reactions by counter reagents when optimized experimental

(3) Iwatsuki, S.; Suzuki, T.; Hasegawa, A.; Funahashi, S.; Kashiwabara, K.; Takagi, H. D. *J. Chem. Soc., Dalton Trans.* **2002**, 3593.

(4) Iwatsuki, S.; Kashiwabara, S.; Kashiwabara, K.; Suzuki, T.; Takagi, H. D. *Dalton Trans.* **2003**, 2280.

(5) (a) Rahman, Md. M.; Liu, H.-Y.; Eriks, K.; Prock, A.; Giering, W. P. *Organometallics* **1989**, *8*, 1. (b) Liu, H.-Y.; Eriks, K.; Prock, A.; Giering, W. P. *Organometallics* **1990**, *9*, 1758.

(6) Bag, N.; Lahiri, G. K.; Chakravorty, A. *J. Chem. Soc., Dalton Trans.* **1990**, 1557.

(7) (a) Pramanik, A.; Bag, N.; Ray, D.; Lahiri, G. K.; Chakravorty, A. *Inorg. Chem.* **1991**, *30*, 410. (b) Pramanik, A.; Bag, N.; Chakravorty, A. *J. Chem. Soc., Dalton Trans.* **1993**, 237.

(8) See Supporting Information for full details.

(9) Altomare, A.; Cascarano, G.; Giacovazzo, C.; Guagliardi, A.; Burla, M. C.; Polidori, G.; Camalli, M. *J. Appl. Crystallogr.* **1994**, *27*, 435.

(10) Sheldrick, G. M. *SHELXL97*; University of Göttingen: Göttingen, Germany, 1997.

Table 1. Crystallographic Data

param	[Ru(EtOCS ₂) ₂ (PPh ₃) ₂]	[Ru(EtOCS ₂) ₂ (PPh ₃) ₂](PF ₆)	[Ru(PrOCS ₂) ₂ (PPh ₃) ₂]	[Ru(PrOCS ₂) ₂ (PPh ₃) ₂](PF ₆)
geometry, solvate	<i>cis</i> -, none	<i>trans</i> -, none	<i>cis</i> -, 0.5CH ₂ Cl ₂ · 0.5CH ₃ CN	<i>trans</i> -, H ₂ O
formula	C ₄₂ H ₄₀ O ₂ P ₂ RuS ₄	C ₄₂ H ₄₀ F ₆ O ₂ P ₃ RuS ₄	C _{45.5} H _{46.5} ClN _{0.5} O ₂ P ₂ RuS ₄	C ₄₄ H ₄₆ F ₆ O ₃ P ₃ RuS ₄
fw	867.99	1012.96	959.03	1059.03
cryst syst	monoclinic	orthorhombic	monoclinic	triclinic
space group, Z	<i>P</i> 2 ₁ / <i>c</i> , 8	<i>P</i> 2 ₁ 2 ₁ 2 ₁ , 4	<i>P</i> 2 ₁ / <i>c</i> , 8	<i>P</i> 1̄, 2
<i>a</i> /Å	11.870(2)	18.622(4)	12.052(5)	11.336(7)
<i>b</i> /Å	36.585(4)	21.445(6)	36.352(14)	11.415(8)
<i>c</i> /Å	20.122(2)	11.089(5)	20.134(9)	19.347(13)
α/deg	90	90	90	76.77(5)
β/deg	101.346(9)	90	100.55(2)	75.76(5)
γ/deg	90	90	90	76.49(5)
<i>V</i> /Å ³	8568(2)	4428(2)	8672(6)	2320(3)
<i>D</i> _{calcd} /Mg m ⁻³	1.346	1.519	1.469	1.516
μ(Mo Kα)/mm ⁻¹	0.669	0.712	0.728	0.684
<i>R</i> ¹ (obsd) ^b	0.053	0.043	0.044	0.074
w <i>R</i> ² (all)	0.210	0.123	0.125	0.224

^a *R*1 = Σ||*F*_o - |*F*_c||/Σ|*F*_o|. ^b *F*_o² > 2σ(*F*_o²). ^c w*R*2 = [Σw(|*F*_o - |*F*_c||)²/Σ|*F*_o|²]^{1/2}.

conditions were chosen. Therefore, the method established by Nicholson and Shain¹¹ was used for the determination of the rate constants of the thermal isomerization process that follows the electrochemical reduction of Ru(III) species (EC process).

The electrochemical measurements and electrolyses of Ru(II) complexes were carried out by a BAS 100B electrochemical analyzer with a glassy carbon disk or fiber as the working electrode, a platinum wire counter electrode, and a Ag/AgNO₃ reference electrode (0.01 mol kg⁻¹ AgNO₃ and 0.1 mol kg⁻¹ tetra-*n*-butylammonium perchlorate in acetonitrile). The temperature of the sample solutions was controlled by circulation of thermostated water. The voltammograms were recorded in reference to the ferrocenium/ferrocene couple. Kinetic measurements, on the basis of the Nicholson and Shain's method,¹¹ were carried out by varying the scanning rate (five different rates from 100 to 1000 mV s⁻¹ were employed) at each temperature. Two electrochemical cells with isothermal and nonisothermal configurations were employed for the measurements, to examine the reversibility of the electrode process.^{12–14} Since the estimated rate constants by using two different cells were identical with each other within the experimental uncertainty, the rate constants for the chemical process that followed the redox reaction at the electrode were confidently determined.

Results and Discussion

Crystal Structures. The crystal structures of all four complexes of [Ru(ROCS₂)₂(PPh₃)₂] and [Ru(ROCS₂)₂(PPh₃)₂](PF₆) (R = Et or Pr) have been determined,⁸ and the molecular structures of the EtOCS₂ complexes are illustrated in Figure 1 (those of the PrOCS₂ complexes are shown in Figure S1 in the Supporting Information). In [Ru(EtOCS₂)₂(PPh₃)₂], the Ru^{II}-S distances for the S atoms located at mutually trans positions to the other S atom are 2.385(2)–2.401(2) Å, while those for the S atoms that are trans to the P atoms are 2.448(2)–2.463(2) Å. Therefore, it appears that there is a significant trans influence by the coordinated P atoms. On the other hand, the P(1)–Ru(1)–S(2) and P(1)–

Ru(1)–S(6) angles are 96.92(8) and 95.04(7)°, respectively, while the P(1)–Ru(1)–S(7) angle is acute at 86.32(7)°. Similarly, P(2)–Ru(1)–S(6) and P(2)–Ru(1)–S(2) angles are larger than the right angle, although the P(2)–Ru(1)–S(1) angle is 86.48(7)°. For the other crystallographically independent molecule, similar features were observed in their bond angles around Ru(51).⁸ Therefore, the two S atoms trans to the PPh₃ ligands are pushed away from the ordinary octahedral apexes by two bulky PPh₃ ligands: the P(1)–Ru(1)–P(2) angle is as wide as 102.17(6)°, although each one of the phenyl rings on two PPh₃ ligands stack through the space to avoid further repulsion between these two unidentate ligands (Figure 1a). The bite angles of two EtOCS₂⁻ ligands are in the range 71.39(6)–71.81(9)°.

In the complex of *trans*-[Ru(EtOCS₂)₂(PPh₃)₂](PF₆) the Ru^{III}-S distances are 2.361(2)–2.372(3) Å that are some 0.028 Å shorter than that for the average Ru^{II}-S distances located at the mutually trans positions: this difference may be taken as the difference in the ionic radii for Ru(II) and Ru(III). The two phosphorus atoms are located along the straight P–Ru–P axis, while four S atoms are positioned in the equatorial plane. The bite angles of two EtOCS₂⁻ ions are 73.12(10) and 73.17(10)°.

The most striking feature observed in the crystal structures of these two complexes in different oxidation states is that the Ru^{III}-P distances in *trans*-[Ru(EtOCS₂)₂(PPh₃)₂](PF₆) [2.441(3) and 2.443(3) Å] are longer than the Ru^{II}-P distances in *cis*-[Ru(EtOCS₂)₂(PPh₃)₂] [2.309(2)–2.315(2) Å] by ca. 0.13 Å. Similarly large differences in the M^{III}-P distances were also observed in the analogous pairs of osmium complexes: *cis*-[Os^{II}(MeOCS₂)₂(PPh₃)₂] (average 2.303(3) Å) vs *trans*-[Os^{III}(MeOCS₂)₂(PPh₃)₂](PF₆) (2.449–(2) Å) and *cis*-[Os^{II}(Et₂NCS₂)₂(PPh₃)₂] (average 2.317(6) Å) vs *trans*-[Os^{III}(Et₂NCS₂)₂(PPh₃)₂](PF₆) (2.439(3) Å).⁷ In those studies the trans isomers of the Os(II) complexes were isolated and the crystal structures were also analyzed; the Os^{II}-P distances in *trans*-[Os^{II}(MeOCS₂)₂(PPh₃)₂] and *trans*-[Os^{II}(Et₂NCS₂)₂(PPh₃)₂] were determined as 2.365(2) and 2.337(8) Å, respectively.⁷ This indicated that the reduction of Os center (from Os^{III} to Os^{II}) in the same coordination environments made remarkable shortening of the Os^{III/II}-P

(11) (a) Bard, A. J.; Faulkner, L. R. *Electrochemical Methods*; John Wiley and Sons: New York, 1980. (b) Nicholson, R. S.; Shain, I. *Anal. Chem.* **1964**, *36*, 706.

(12) Yee, E. L.; Cave, R. J.; Guyer, K. L.; Tyma, P. D.; Weaver, M. J. *J. Am. Chem. Soc.* **1979**, *101*, 1131.

(13) Criss, C. M.; Salomom, M. *Physical Chemistry of Organic Solvent Systems*; Covington, A. K., Dickinson, T., Eds.; Plenum Press: New York, 1973.

(14) Agar, J. N. *Adv. Electrochem. Eng.* **1963**, *3*, 31.

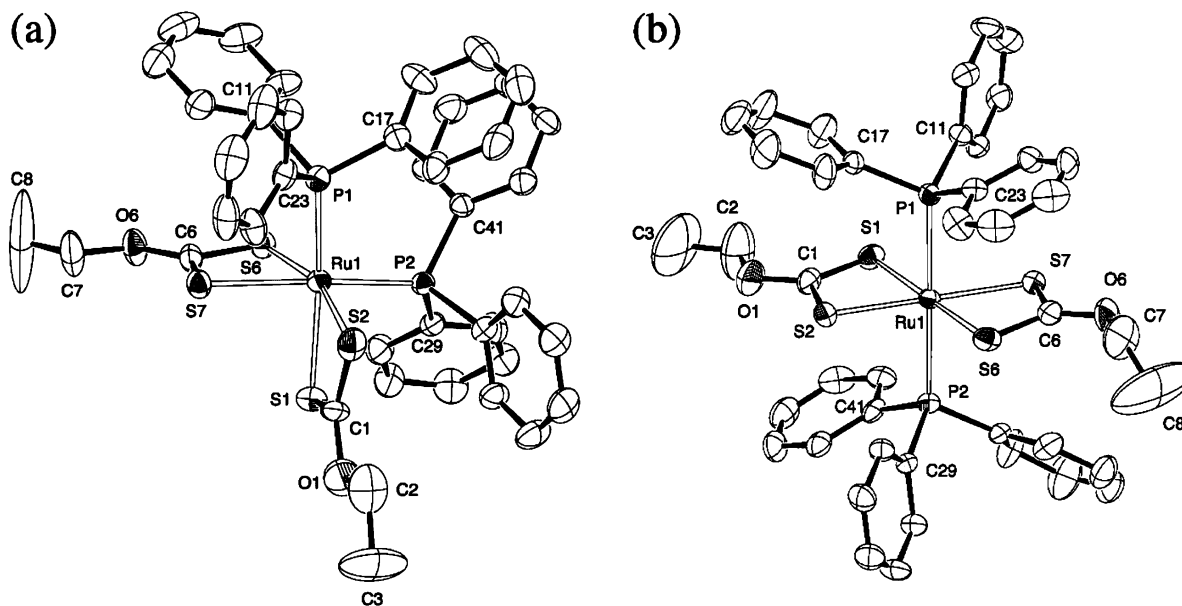


Figure 1. ORTEPs (30% probability level, hydrogen atoms omitted). Selected bond lengths (Å) and angles (deg) for (a) one of the crystallographically independent complex molecules in *cis*-[Ru(EtOCS₂)₂(PPh₃)₂], Ru(1)–P(1) 2.315(2), Ru(1)–P(2) 2.309(2), Ru(1)–S(1) 2.452(2), Ru(1)–S(2) 2.397(2), Ru(1)–S(6) 2.385(2), Ru(1)–S(7) 2.463(2), P(1)–Ru(1)–P(2) 102.17(6), S(1)–Ru(1)–S(2) 71.81(9), and S(6)–Ru(1)–S(7) 71.39(6), and (b) the cationic part in *trans*-[Ru(EtOCS₂)₂(PPh₃)₂](PF₆), Ru(1)–P(1) 2.443(3), Ru(1)–P(2) 2.441(3), Ru(1)–S(1) 2.371(3), Ru(1)–S(2) 2.363(3), Ru(1)–S(6) 2.372(3), Ru(1)–S(7) 2.361(2), P(1)–Ru(1)–P(2) 179.63(9), S(1)–Ru(1)–S(2) 73.12(10), and S(6)–Ru(1)–S(7) 73.17(10).

bonds as a result of a large augmentation of $5d\pi-3d\pi$ back-bonding.⁷ In contrast, in the Ru^{III/II} complexes having a similar coordination environment, the Ru–P bonds were not so sensitive to the oxidation state of Ru center; i.e., the Ru^{III}–P bonds in *trans*(*P*)-[RuCl₂(O₂CPh)(PPh₃)₂] (2.414 Å) are comparable to the Ru^{II}–P bonds in *trans*(*P*)-[RuCl(CO)(O₂CPh)(PPh₃)₂] (2.410 and 2.374 Å).¹⁵ A very recent example of [Ru^{III/II}(dppbt-O₂)₂(dppbt)]^{−0} (dppbt = 2-(diphenylphosphino)benzenethiolate; dppbt-O₂ = 2-(diphenylphosphino)benzenesulfinate) also showed similar Ru^{III/II}–P distances between the Ru(II) and Ru(III) complexes.¹⁶ Hence, for the Ru^{III/II}–P bonds the contribution of $4d\pi-3d\pi$ back-bonding remained unaltered by the difference in the oxidation state of Ru center (e.g., Ru(II)- d^5 or Ru(III)- d^6). Although we could not isolate (and, therefore, not determine the structure of) the *trans* isomer of the Ru(II) complex, *trans*-[Ru^{II}(EtOCS₂)₂(PPh₃)₂], it is, therefore, claimed that a remarkable elongation of the Ru^{III}–P bonds in *trans*-[Ru^{III}(EtOCS₂)₂(PPh₃)₂](PF₆) as compared to the Ru^{II}–P bonds in *cis*-[Ru^{II}(EtOCS₂)₂(PPh₃)₂] results from a large mutual *trans* influence of PPh₃; it seems that the difference in the degree of the $5d\pi-3d\pi$ and $4d\pi-3d\pi$ interaction originates from the relativistic effect,² which is effective especially for the third-row transition elements such as Os.

In conclusion, the mutual *trans* influence of PPh₃ in the Ru(III) complexes is as large as that in the analogous Ru(II) complexes and the *trans* coordination geometry in [Ru(EtOCS₂)₂(PPh₃)₂](PF₆) is caused essentially by the large steric repulsion between two PPh₃ and smaller ionic size of Ru(III). Complexes of [Ru(ⁱPrOCS₂)₂(PPh₃)₂]⁺⁰ exhibited

structural features similar to those of the [Ru(EtOCS₂)₂(PPh₃)₂]⁺⁰ complexes.⁸

Stability of the Transient *trans*-Ru(II) Species in Dichloromethane. As a preliminary experiment, we examined the rate constant for the chemical process that followed the electrochemical reduction of *trans*-[Ru(ⁱPrOCS₂)₂(PPh₃)₂]⁺ at ambient temperature with varying the concentration of PPh₃ in the bulk: the observed rate constant for the thermal isomerization of *trans*-[Ru(ⁱPrOCS₂)₂(PPh₃)₂] to *cis*-[Ru(ⁱPrOCS₂)₂(PPh₃)₂] (vide infra) decreased with increasing [PPh₃]_{free} up to [PPh₃]_{free} = 20 mmol kg^{−1}, while further addition of excess PPh₃ in the bulk (>20 mmol kg^{−1}) gradually accelerated decomposition of *trans*-[Ru(ⁱPrOCS₂)₂(PPh₃)₂], which was observed by the complete loss of typical absorption bands of the expected product, *cis*-Ru(II). This observation indicates that a large excess PPh₃ in the bulk induces decomposition of the transient *trans*-Ru(II) species, while no appreciable degree of decomposition was observed when less than 10 mmol kg^{−1} of free PPh₃ was added. Therefore, we used experimental conditions $0 \leq [\text{PPh}_3] \leq 10 \text{ mmol kg}^{-1}$ to investigate the effect of free PPh₃ in the bulk on the thermal isomerization reactions of *trans*-[Ru(ⁱPrOCS₂)₂(PPh₃)₂], to avoid appreciable amounts of decomposition of the intermediate during the observation of the isomerization process. As for *trans*-[Ru(EtOCS₂)₂(PPh₃)₂], the decomposition induced by PPh₃ in the bulk was the more evident even at [PPh₃] = 10 mmol kg^{−1}. Because of this instability, it was not possible to examine the isomerization kinetics involving transient *trans*-[Ru(EtOCS₂)₂(PPh₃)₂]. Results of the preliminary experiment indicate that the decomposition of the transient *trans*-Ru(II) species induced by excess PPh₃ in the bulk is associative in nature, since ⁱPrOCS₂[−] is somewhat more bulky compared with EtOCS₂[−]. On the other hand, *cis*-Ru(II) complexes are indefinitely

(15) (a) McGuiggan, M. F.; Pignolet, L. H. *Cryst. Struct. Commun.* **1978**, *7*, 583. (b) McGuiggan, M. F.; Pignolet, L. H. *Cryst. Struct. Commun.* **1981**, *10*, 1227.

(16) Grapperhaus, C. A.; Poturovic, S.; Mashuta, M. S. *Inorg. Chem.* **2005**, *44*, 8185.

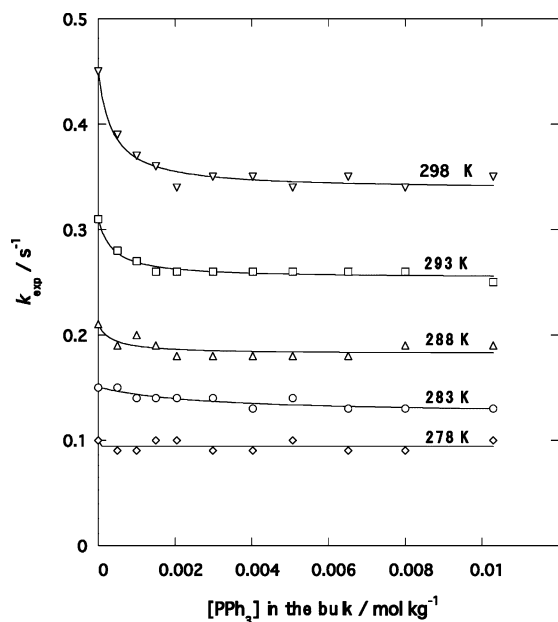


Figure 2. Dependence of k_{exp} on $[\text{PPh}_3]$ at various temperatures. Curved lines at each temperature represent the calculated points on the basis of the data in Tables 2 and S4, by using eq 4. $[\text{Ru}^{\text{III}}] = 1.0 \text{ mmol kg}^{-1}$, and $I = 0.1 \text{ mol kg}^{-1}$ $[\text{TBAPF}_6]$.

stable in dichloromethane solution at room temperature and decomposition was not induced for *cis*-Ru(II) complexes even with a large excess of free PPh₃ in the bulk.

Kinetic Analyses of the Thermal Reactions Involving Transient *trans*-[Ru(ⁱPrOCS₂)₂(PPh₃)₂] Species in Dichloromethane. Reactions of the transient species, *trans*-[Ru(ⁱPrOCS₂)₂(PPh₃)₂], produced by the electrochemical reduction of *trans*-[Ru(ⁱPrOCS₂)₂(PPh₃)₂]⁺ were examined at various temperatures. Chakravorty et al. postulated that the disappearance of the transient [Ru(ROCS₂)₂(PPh₃)₂] complexes (R = Me and ⁱPr) produced at the electrode was attributed only to the trans to cis isomerization process and reported that the reactions proceeded through the intramolecular twist mechanism without giving sufficient reasons.⁶ the reported activation parameters were $\Delta H^* = 46.6 \text{ kJ mol}^{-1}$, $\Delta S^* = -96.6 \text{ J mol}^{-1} \text{ K}^{-1}$, and $k = 0.15 \text{ s}^{-1}$ (283 K) for R = Me and 40.7 kJ mol^{-1} , $-122.6 \text{ J mol}^{-1} \text{ K}^{-1}$, and $k = 0.095 \text{ s}^{-1}$ (283 K) for R = ⁱPr. As discussed in our previous articles,^{3,4} dissociation of coordinated phosphine ligands may also have to be taken into account for the complete analyses of such isomerization processes. Therefore, we reinvestigated the trans to cis isomerization rate for the [Ru(ⁱPrOCS₂)₂(PPh₃)₂] complexes, by using the method identical with that employed by Chakravorty et al. Cyclic voltammograms exhibited by *cis*-[Ru(ⁱPrOCS₂)₂(PPh₃)₂] and *trans*-[Ru(ⁱPrOCS₂)₂(PPh₃)₂]⁺ in dichloromethane were quite similar to those reported by Chakravorty et al.⁶

As shown in Figure 2 (averaged values of rate constants at each condition are summarized in Table S4 in the Supporting Information), the rate constant for the chemical process that followed the electrochemical reduction of *trans*-[Ru(ⁱPrOCS₂)₂(PPh₃)₂]⁺ decreased to a constant value at higher concentration of added PPh₃ (up to ca. 10 mmol kg^{-1} , as described in the previous section). Such a dependence of

Table 2. Isolated Values of k_1 , k_3 , and the Ratio of k_2/k_{-1} at Various Temperatures and the Activation Parameters for k_1 and k_3

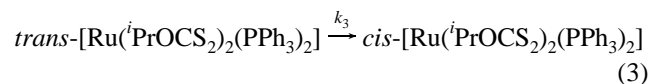
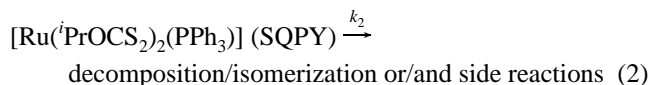
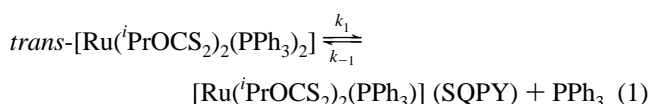
T/K^a	$10^2 k_1/\text{s}^{-1}$	k_3/s^{-1}	$(k_{-1}/k_2)/\text{kg mol}^{-1} b$
278.3	1.72 ± 1.44	0.077 ± 0.014	1210 ± 9800
283.3	2.63 ± 0.57	0.124 ± 0.006	363 ± 278
288.3	2.79 ± 0.72	0.182 ± 0.004	2750 ± 2690
293.3	5.63 ± 0.40	0.254 ± 0.002	2740 ± 728
298.3	11.3 ± 0.8	0.338 ± 0.004	2340 ± 734

Activation Parameters^c

$\Delta H^* = 97.6 \pm 0.8 \text{ kJ mol}^{-1}$; $\Delta S^* = 64 \pm 3 \text{ J mol}^{-1} \text{ K}^{-1}$ for k_1
 $\Delta H^* = 41.8 \pm 1.5 \text{ kJ mol}^{-1}$; $\Delta S^* = -114 \pm 7 \text{ J mol}^{-1} \text{ K}^{-1}$ for k_3

^a Temperature was controlled by circulation of thermostated water within $\pm 0.2 \text{ K}$. ^b Although errors for k_{-1}/k_2 at each temperature are very large, the k_1 and k_3 (especially k_3) values were not sensitive to the ratio of k_{-1}/k_2 . ^c The activation parameters were determined without using data obtained at low temperatures (278.3 and 283.3 K).

apparent rate constant on the concentration of PPh₃ in the bulk may indicate the involvement of the dissociative isomerization/decomposition process other than the intramolecular isomerization process, as described by the following equations:^{3,4,17}



The apparent rate constant, k_{exp} , that corresponds to the disappearance of transient *trans*-[Ru(ⁱPrOCS₂)₂(PPh₃)₂] is then expressed by eq 4, by assuming a steady state for the five-coordinate pseudo-square pyramidal (SQPY = C_{2v}) species,

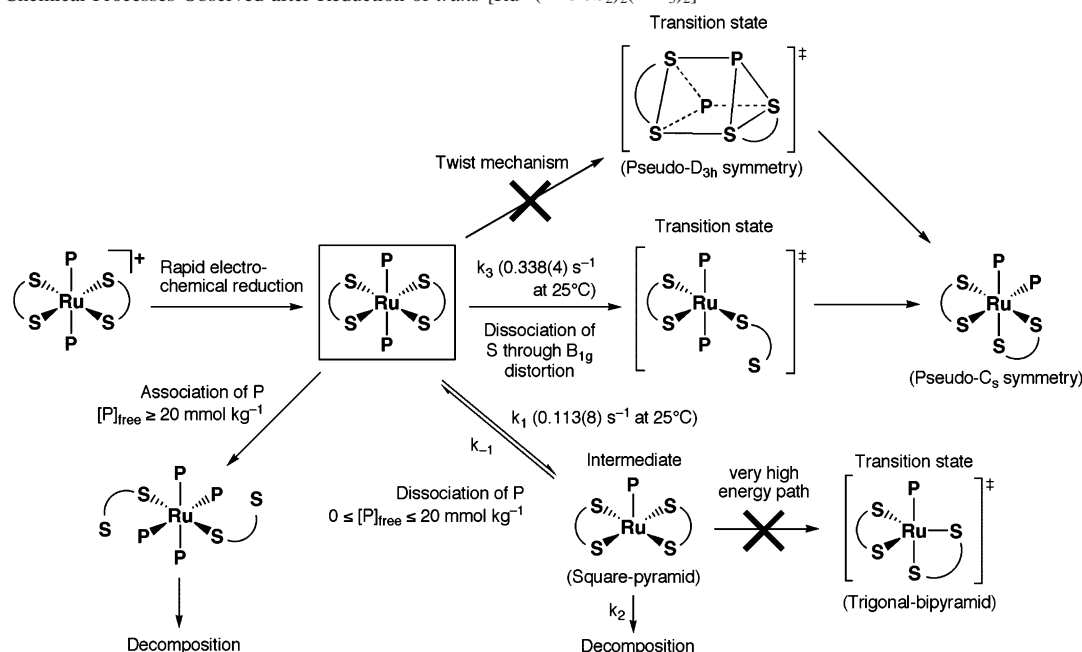
$$-\frac{d[\text{trans-}[\text{Ru}(\text{}^i\text{PrOCS}_2)_2(\text{PPh}_3)_2]]}{dt} = k_{\text{exp}}[\text{trans-}[\text{Ru}(\text{}^i\text{PrOCS}_2)_2(\text{PPh}_3)_2]]$$

$$k_{\text{exp}} = \frac{k_2(k_1 + k_3) + k_3k_{-1}[\text{PPh}_3]_{\text{free}}}{(k_{-1}[\text{PPh}_3]_{\text{free}} + k_2)}$$

$$= \frac{k_1 + k_3 + k_3A[\text{PPh}_3]_{\text{free}}}{(A[\text{PPh}_3]_{\text{free}} + 1)} \quad (4)$$

where $[\text{PPh}_3]_{\text{free}}$ is the concentration of excess free PPh₃ in the bulk and $A = k_{-1}/k_2$. The curvature of the plots in Figure 2 indicates that the A value is in the order of 10^3 , since $A[\text{PPh}_3]_{\text{free}}$ in the denominator is not significantly different from unity when $[\text{PPh}_3]_{\text{free}} \approx 10 \text{ mmol kg}^{-1}$. The results obtained by the least-squares analyses are summarized in Table 2. Since the dependency of k_3 on the other rate constants was small (as judged from the dependency factor given by the “Sigma Plot” program), the activation param-

(17) Jordan, R. B. *Reaction Mechanisms of Inorganic and Organometallic Systems*, 2nd ed.; Oxford Press: New York, 1998.

Scheme 1. Chemical Processes Observed after Reduction of $trans\text{-}[\text{Ru}^{\text{III}}(\text{PrOCS}_2)_2(\text{PPh}_3)_2]^+$ 

eters for the k_3 process were confidently determined as $\Delta H^* = 41.8 \pm 1.5 \text{ kJ mol}^{-1}$ and $\Delta S^* = -114 \pm 7 \text{ J mol}^{-1} \text{ K}^{-1}$ by using data at $T > 288 \text{ K}$ (the activation parameters estimated by using data obtained at all temperatures were $\Delta H^* = 48.4 \pm 2.4 \text{ kJ mol}^{-1}$ and $\Delta S^* = -91.2 \pm 9 \text{ J mol}^{-1} \text{ K}^{-1}$, showing limited dependence of k_3 on the other rate constants). On the other hand, the k_1 value became unreliable at low temperatures since it depended largely on the k_3 value. The activation parameters for the k_1 process were determined as $\Delta H^* = 97.6 \pm 0.8 \text{ kJ mol}^{-1}$ and $\Delta S^* = 64 \pm 3 \text{ J mol}^{-1} \text{ K}^{-1}$ (only data obtained at $T \geq 288.3 \text{ K}$ were used). The values of k_1 and k_3 were $0.113 \pm 0.008 \text{ s}^{-1}$ and $0.338 \pm 0.004 \text{ s}^{-1}$, respectively, for the reactions of transient $trans\text{-}[\text{Ru}^{\text{II}}(\text{PrOCS}_2)_2(\text{PPh}_3)_2]$ at 25 °C (Scheme 1).

In the previous study, it was reported that the isomerization process through the five coordinate intermediate was very slow because of the high energy barrier for the $[\text{Co}(\text{dtc})_2(\text{P-ligands})_2]^+$ complex (dtc = *N,N*-dimethyldithiocarbamate, and P-ligand = unidentate phosphines or phosphites), on the basis of the AOM calculation.^{3,4} Such a high activation energy for the structural change from pseudo-square pyramidal structure (SQPY) to the pseudo-trigonal bipyramidal transition state was explained by the relatively large π -acidity of the ligands.¹⁸ Since the $10Dq$ value is somewhat larger for $[\text{Ru}^{\text{II}}(\text{PrOCS}_2)_2(\text{PPh}_3)_2]$ than that for $[\text{Co}(\text{dtc})_2(\text{P-ligand})_2]^+$ and since the interelectronic repulsion parameters (Racah's *B* and *C* parameters) are significantly smaller for the complexes of second-row transition metals, the activation enthalpy expected for the change from the five-coordinate pseudo-square pyramidal to pseudo-trigonal bipyramidal structure should be much larger for $[\text{Ru}^{\text{II}}(\text{PrOCS}_2)_2(\text{PPh}_3)_2]$ than that for the corresponding $\text{Co}(\text{III})$ complex with dtc⁻ ligands: isomerization through the k_2 process does not take

place for these $\text{Ru}(\text{II})$ complexes;^{3,4,18} the k_2 process merely leads to the decomposition of the five-coordinate species.

Although kinetic data reported for solvent exchange and ligand substitution reactions are scarce, the ligand substitution reactions in $\text{Ru}(\text{II})$ complexes have been considered to occur through the dissociative interchange mechanism.¹⁹ The k_1 value for the $[\text{Ru}^{\text{II}}(\text{PrOCS}_2)_2(\text{PPh}_3)_2]$ complex obtained in this study is more than 10 times larger than the water exchange rate constant in hexaaquaruthenium(II), 0.018 s^{-1} at 298 K.²⁰ On the other hand, a *trans*-labilization effect by the coordination of η^6 -benzene in $[\text{Ru}(\eta^6\text{-C}_6\text{H}_6)(\text{OH}_2)_3]^{2+}$ was reported by Merbach and co-workers, in which the water exchange rate constant was accelerated to $11.5 \pm 3.1 \text{ s}^{-1}$ at 298 K.^{19b} It seems that the $\text{Ru}^{\text{II}}\text{-P}$ bond energy is not small despite the expected large mutual *trans* influence/*trans* effect of the PPh_3 ligand coordinated at the mutually *trans* positions in $trans\text{-}[\text{Ru}^{\text{II}}(\text{PrOCS}_2)_2(\text{PPh}_3)_2]$, k_1 is not significantly large. Such a stabilization of $\text{Ru}^{\text{II}}\text{-P}$ bonds in $trans\text{-}[\text{Ru}^{\text{II}}(\text{PrOCS}_2)_2(\text{PPh}_3)_2]$ may be explained either by the electronic sponge effect of the spectator ligand,^{3,4} PrOCS_2^- , or by the intrinsic strength of the $\text{Ru}^{\text{II}}\text{-P}$ bond.

As the replacement of a coordinated ligand through the associative attack by free PPh_3 leads to the decomposition of these complexes with a more rapid rate (see previous section), such a process involves the dissociation of coordinated dithiocarbonate ligand (Scheme 1). According to the second-order perturbation theory [symmetry rules and the principle of the least motion (=PLM)],²¹ a mixing of A_{1g} and B_{1g} states causes asymmetric elongation of $\text{Ru}^{\text{II}}\text{-S}$ bonds through the B_{1g} mode of vibration, for the d^6 configuration

(18) (a) Vanquickenborne, L. G.; Pierloot, K. *Inorg. Chem.* **1981**, *20*, 3673.
 (b) Vanquickenborne, L. G.; Pierloot, K. *Inorg. Chem.* **1984**, *23*, 1471.

(19) (a) Richens, D. T. *The Chemistry of Aqua Ions*; Wiley: New York, 1997. (b) Stebler-Rothlisberger, M.; Hummel, W.; Pittet, P.-A.; Burgi, H.-B.; Ludi, A.; Merbacher, A. E. *Inorg. Chem.* **1988**, *27*, 1358.
 (20) Wilkins, R. G. *Kinetics and Mechanism of Reactions of Transition Metal Complexes*, 2nd ed.; VCH: New York, 1991.

in the D_{2h} symmetry. Incoming free PPh₃ ligand at the xy plane is expected to induce this mixing by lowering the LUMO level. Such a process is the more favored by *trans*-[Ru(EtOCS₂)₂(PPh₃)₂] than the ⁱPr derivative, because of the less steric hindrance of this dithiocarbonate ligand.

On the other hand, it was found that *cis*-Ru(II) complexes are indefinitely stable in dichloromethane solution while *trans*-Ru(III) complexes gradually decomposed at room temperature, although it took more than 12 h before obvious decomposition was observed for the latter complexes in solution. It should also be noted that decomposition was not induced for *cis*-Ru(II) complex even with excess free PPh₃. Since the dissociation of coordinated PPh₃ is typical only for the *trans*-Ru(II) and *trans*-Ru(III) species, it is concluded that the dissociation of coordinated PPh₃ from *trans*-Ru(II) complex is a result of the *trans* effect. Therefore, the slow dissociation of coordinated PPh₃ from *trans*-[Ru(ⁱPrOCS₂)₂(PPh₃)₂] under the conditions of [PPh₃]_{free} < 10 mmol kg⁻¹ is considered to take place by the *limiting* dissociative mechanism (destabilization of the ground state). The large activation enthalpy and the large positive activation entropy estimated for the k_1 process support this conclusion.

For the k_3 (isomerization) process, the activation entropy was largely negative. The large negative entropy observed for the k_3 process in the case of *trans*-Ru(II) complex indicates that the reaction proceeds through a transition state with a larger polarity than in the ground state: a charge separation process is invoked. As discussed above, the dissociative isomerization pathway that involves the change from pseudo-square planar to pseudo-trigonal bipyramidal structure does not take place for Ru(II) (and Co(III) complexes), since such a structural change requires rather high energy (Scheme 1). On the other hand, it has been known that the stability constants of the transition metal complexes with dithiocarbonate and dithiocarbamate ligands depend largely on the size and charge of the metal ion.²² Therefore, it is certain that the energy of the Ru^{II}–S bond is much smaller than that for the Co^{III}–S bond. As a result,

- (21) (a) Burdett, J. K. *Molecular Shapes: Theoretical Models of Inorganic Stereochemistry*; John Wiley and Sons: New York, 1980. (b) Itoh, S.; Kishikawa, N.; Suzuki, T.; Takagi, H. D. *Dalton Trans.* **2005**, 1066 and references therein.
(22) Sillen, L. G. *Stability Constants of Metal-Ion Complexes*; Royal Society of Chemistry: London, 1971.

the Ru^{II}–S bond is expected to ramble through the low-energy B_{1g} mode of vibration, although the ligand may not completely dissociate from the metal center (Scheme 1). A rather large rate constant, k_3 (small activation enthalpy), together with the large negative activation entropy for this process, strongly indicates that the intramolecular isomerization reaction proceeds through the $D_{2h} \rightarrow C_s$ structural change (through the allowed B_{1g} mode of partial dissociation of one of the Ru^{II}–S bonds, according to the symmetry rules and PLM as described above), for which the free energy barrier should not be large since the resulting *cis* conformation is also in the pseudo- C_s symmetry. The large negative activation entropy is attributed to the increased electrostriction caused by the charge separation that occurs during this process.

Conclusion

Crystal structures of [Ru(EtOCS₂)₂(PPh₃)₂]⁺⁰ and [Ru(ⁱPrOCS₂)₂(PPh₃)₂]⁺⁰ pairs were determined for the first time; in the Ru(III) complexes the coordination structures around Ru(III) were in the D_{2h} symmetry with elongated Ru^{III}–P bonds because of the mutual *trans* influence, while two PPh₃ molecules in the corresponding Ru(II) species were observed at the *cis* positions. From the analyses of the EC reactions, rate constants for the *trans* to *cis* isomerization in [Ru(ⁱPrOCS₂)₂(PPh₃)₂] and the dissociation reaction of the coordinated PPh₃ ligand were isolated for the first time. It was shown that the latter process takes place by the *limiting* dissociative mechanism, while the former process proceeds through dissociation of one of the Ru^{II}–S bonds. The slow dissociative activation of PPh₃ from transient *trans*-[Ru(ⁱPrOCS₂)₂(PPh₃)₂] indicates the mild mutual *trans* effect in d⁶-Ru(II), while the elongation of the Ru(III)–P bonds in *trans*-[Ru(ⁱPrOCS₂)₂(PPh₃)₂]⁺ was attributed to the mutual *trans* influence since decomposition of this species was much slower.

Supporting Information Available: Experimental procedures including syntheses, crystallography, and spectroscopic measurements of the complexes, ORTEPs, and UV–vis absorption spectra of the ⁱPrOCS₂ complexes and the table of rate constants at each condition measured (PDF/CIF format). This material is available free of charge via the Internet at <http://pubs.acs.org>.

IC051487L